The tight junction protein complex undergoes rapid and continuous molecular remodeling at steady state

Le Shen, Christopher R. Weber, and Jerrold R. Turner

Department of Pathology, The University of Chicago, Chicago, IL 60637

The tight junction defines epithelial organization. Structurally, the tight junction is comprised of transmembrane and membrane-associated proteins that are thought to assemble into stable complexes to determine function. In this study, we measure tight junction protein dynamics in live confluent Madin–Darby canine kidney monolayers using fluorescence recovery after photobleaching and related methods. Mathematical modeling shows that the majority of claudin-1 (76 ± 5%) is stably localized at the tight junction. In contrast, the majority of occludin (71 ± 3%) diffuses rapidly within the tight junction with a diffusion constant of 0.011 $\mu m^2 s^{-1}$. Zonula occludens-1 molecules are also highly dynamic in this region, but, rather than diffusing within the plane of the membrane, 69 ± 5% exchange between membrane and intracellular pools in an energy-dependent manner. These data demonstrate that the tight junction undergoes constant remodeling and suggest that this dynamic behavior may contribute to tight junction assembly and regulation.

Introduction

The epithelial tight junction, or zonula occludens (ZO), separates apical and basolateral plasma membrane domains and serves as a selectively permeable barrier to regulate paracellular diffusion (Farquhar and Palade, 1963; Claude and Goodenough, 1973). More than 30 integral and peripheral membrane proteins targeted to the tight junction have been identified (Stevenson et al., 1986; Citi et al., 1988; Furuse et al., 1993, 1998; Itoh et al., 1993; Jesaitis and Goodenough, 1994; Zahraoui et al., 1994; Dodane and Kachar, 1996; Haskins et al., 1998; Izumi et al., 1998; Martin-Padura et al., 1998; Chen and Lu, 2003; Hurd et al., 2003; Kohler et al., 2004; Ohnishi et al., 2004; Tomson et al., 2004; Ikenouchi et al., 2005). ZO-1, the first tight junction protein identified (Stevenson et al., 1986), includes three tandem PDZ protein interaction domains that mediate binding to other plaque and transmembrane tight junction proteins (Beatch et al., 1996; Haskins et al., 1998; Itoh et al., 1999; Ebnet et al., 2000; Bezprozvanny and Maximov, 2001; Hamazaki et al., 2002; Fanning et al., 2007). In addition, ZO-1 and the structurally related proteins ZO-2 and -3 interact with perijunctional filamentous actin both directly and indirectly through other proteins such as α-catenin and cingulin, thereby anchoring the tight junc-

tion to the cytoskeleton (Rajasekaran et al., 1996; Itoh et al., 1997; Fanning et al., 1998; Cordenonsi et al., 1999; Wittchen et al., 1999; Bazzoni et al., 2000; Fanning et al., 2002). Claudins bind ZO-1, -2, and -3 via a C-terminal PDZ-binding motif (Itoh et al., 1999). The importance of this interaction is demonstrated by the association of a ZO-2 mutation that reduces claudin binding with familial hypercholanemia (Carlton et al., 2003) as well as a study of cells lacking ZO-1 and -2, which fail to recruit claudins and do not develop barrier function (Umeda et al., 2006).

Together with the functional importance of claudin–ZO-1/-2 interactions, the multitude of interactions among tight junction proteins demonstrated by in vitro binding assays and coimmunoprecipitation studies (Balda et al., 1996; Fanning et al., 1998; Mitic and Anderson, 1998; Cordenonsi et al., 1999; Bazzoni et al., 2000; Kale et al., 2003; Van Itallie and Anderson, 2004; Li et al., 2005) has led to the hypothesis that the steady-state tight junction is a large complex maintained by abundant protein cross-links. By analogy, this model is supported by a recent study of the adherens junction that demonstrates that epithelial cadherin, α-catenin, and β-catenin form a stable complex with one another (Yamada et al., 2005). However, only one study has directly assessed the dynamic behavior of tight junction proteins in the absence of external stimuli. That work concluded that fluorescent-tagged claudin-1 expressed in fibroblasts is not mobile within the tight junction–like strands that develop in

Correspondence to Jerrold R. Turner: jturner@bsd.uchicago.edu

Abbreviations used in this paper: FLIP, fluorescent loss in photobleaching; MBCD, methyl-β-cyclodextrin; PA, photoactivable; TER. transepithelial resistance; ZO, zonula occludens.
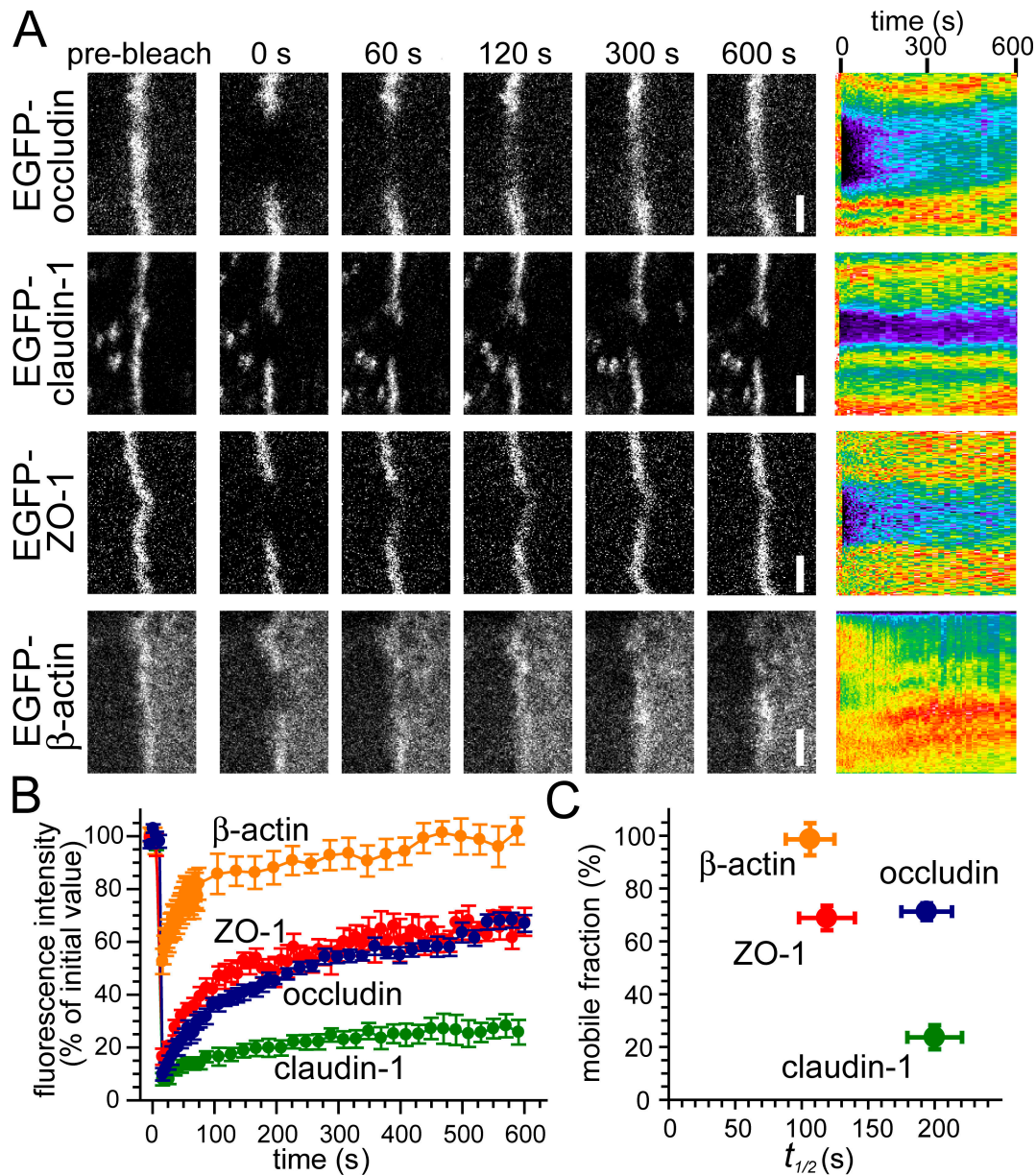
Figure 1. **Individual tight junction proteins display distinct FRAP behaviors in polarized epithelia.** (A) EGFP-occludin, –claudin-1, –ZO-1, and –β-actin were studied by FRAP. High magnification images of tight junction segments before and at the indicated time points after photobleaching are shown in the left panels. Corresponding kymographs are shown at the right. (B) Quantitative analysis of FRAP from experiments similar to those shown in B (n = 7, 6, 8, and 6 for occludin, claudin-1, ZO-1, and β-actin, respectively). (C) The mobile fraction and $t_{1/2}$ of recovery for each protein were calculated from the recovery curves in B. Error bars represent SEM. Bars, 2 μm.

these cells (Sasaki et al., 2003). Thus, the tight junction is widely viewed as a static structure under steady-state conditions.

Our study of fluorescent tight junction fusion proteins expressed in epithelial monolayers raised the possibility of occludin flow within the tight junction (Shen and Turner, 2005). Although this observation could represent the flow of tight junction protein complexes, as occurs for cadherin–catenin complexes at the adherens junction, it could also suggest that binding interactions at the tight junction are far more dynamic than previously thought. Therefore, we directly assessed protein dynamics within the tight junction and now show that tight junction proteins are highly dynamic in resting steady-state epithelial monolayers. Each protein studied displays distinct dynamic behavior, reflecting different mechanisms

of protein movement. These data demand that our current model of tight junction molecular structure be revised and may provide a basis for understanding the mechanisms that allow rapid tight junction remodeling in response to extracellular stimuli.

Results

The multiprotein complex within the tight junction is dynamic at steady state

We recently reported the generation and validation of ZO-1, occludin, and claudin-1 fluorescent fusion proteins using EGFP and monomeric RFP1 (Shen and Turner, 2005). Each of these fusion proteins is accurately targeted to the tight junction and localizes

with the corresponding endogenous protein, as assessed biochemically and morphologically at steady state and in response to stimuli (Shen and Turner, 2005). Moreover, expression of these fusion proteins does not disrupt normal function either in vitro (Shen and Turner, 2005) or in vivo (unpublished data). Therefore, we conclude that these fluorescent fusion proteins are suitable tools for analysis of tight junction protein dynamics in live cells.

Time-lapse imaging of confluent MDCK epithelial cell monolayers expressing fluorescent-tagged occludin frequently demonstrated small fluctuations in fluorescent intensity despite stable barrier function (Shen and Turner, 2005). Although such fluctuations were not seen in fixed monolayers, they could potentially represent imaging artifacts as a result of slight movements of live cells within the z plane. To distinguish between artifact and actual movement of occludin within the tight junction, occludin dynamics were assessed by monitoring FRAP in confluent monolayers with established intercellular junctions. These experiments show that the majority of tight junction–associated occludin is available for exchange; the mobile fraction is $71 \pm 3\%$ (Fig. 1, A–C). This observation was unexpected because occludin interacts with many proteins at the tight junction, and the generally accepted model of steady-state tight junction structure is of a highly stable multiprotein complex (Chen et al., 1997; Gonzalez-Mariscal et al., 2000; Tsukita et al., 2001; Peng et al., 2003; Seth et al., 2007).

Because occludin exchange occurs relatively slowly with a $t_{1/2}$ of 194 ± 19 s, the observed FRAP could represent diffusion of an occludin-containing protein complex within the tight junction. To determine whether tight junction proteins remain bound to one another during exchange, the mobility of ZO-1, which binds directly to occludin, was assessed (Furuse et al., 1994; Fanning et al., 1998; Schmidt et al., 2001; Li et al., 2005). Similar to occludin, $69 \pm 5\%$ of tight junction–associated ZO-1 is available for exchange (Fig. 1, A–C). However, unlike occludin, ZO-1 exchanges more rapidly, with a $t_{1/2}$ of only 119 ± 21 s. Thus, despite well-characterized binding interactions between ZO-1 and occludin, these data suggest that there is a continuous and rapid dissociation of the majority of each of these proteins from one another within fully assembled steady-state tight junctions.

The unexpected differences in FRAP kinetics between ZO-1 and occludin prompted investigation of the exchange kinetics of claudin-1 and tight junction–associated β-actin. Claudin-1 has a small mobile fraction of $24 \pm 5\%$ (Fig. 1, A–C). Thus, in contrast to occludin and ZO-1, only a minority of tight junction–associated claudin-1 undergoes exchange at the tight junction. Consistent with reports that actin is highly dynamic at cell–cell contact sites (Yamada et al., 2005), the majority of junction-associated β-actin exchanges rapidly with a mobile fraction of $98 \pm 6\%$ and a $t_{1/2}$ of 106 ± 18 s. Remarkably, the combination of mobile fraction and $t_{1/2}$ of fluorescent recovery is unique for each of these four representative proteins (Fig. 1 C).

Recent work suggests that interactions between claudin proteins and ZO-1 or -2 are necessary for tight junction assembly (Umeda et al., 2006) and that the stability of steady-state tight junction function increases with the duration of postconfluent monolayer culture (Tang and Goodenough, 2003). Therefore, it is possible that the aforementioned distinct FRAP behaviors may differ if

Table I. **The dynamic behavior of tight junction proteins changes after confluence**

|	Postconfluent time	Mobile fraction	$t_{1/2}$
	d	%	s
Occludin			
	1	74 ± 7	139 ± 17
	3	71 ± 3	194 ± 19
	10	77 ± 3	107 ± 8[a]
Claudin-1			
	1	25 ± 3	142 ± 36
	3	24 ± 5	200 ± 21
	10	22 ± 2	195 ± 65
ZO-1			
	1	87 ± 5[a]	101 ±1 5
	3	69 ± 5	119 ± 21
	10	72 ± 3	98 ± 16
β-Actin			
	1	99 ± 2	15 ± 1[a]
	3	99 ± 6	106 ± 18
	10	97 ± 3	43 ± 8[a]

All measurements represent means of at least five independent measurements.
[a]P < 0.05 versus 3-d monolayers.

studied shortly or at prolonged intervals after confluence. To assess this, FRAP behaviors of occludin, claudin-1, ZO-1, and β-actin were measured in monolayers 1, 3, and 10 d after confluence, representing steady-state kinetics present in newly formed (1 d), assembled (3 d), and older, stable (10 d) MDCK monolayers (Table I). At 1 d after confluence, the increased ZO-1 mobile fraction and decreased β-actin $t_{1/2}$, both relative to values at 3 d, suggest that the assembling tight junction is highly dynamic. Although the tight junction is far more stable at 3 d after confluence, there is an increase in dynamic behavior 10 d after confluence that is manifested as reduced $t_{1/2}$ for both occludin and tight junction–associated β-actin (Table I). Although the significance of this late increase in exchange rates is not clear, it is possible that the structure of the fully mature tight junction is specially modified to allow rapid regulation and fine-tuning of function. In any case, these data demonstrate that in stark disagreement with prevailing models of the tight junction, the multiprotein complex within the tight junction is highly dynamic at steady state.

Occludin and ZO-1 exchange are differentially dependent on membrane properties and metabolic energy

To begin to dissect processes that mediate tight junction protein exchange, monolayers were subjected to treatments that broadly affect cellular functions. Initially, the temperature dependence of occludin and ZO-1 FRAP behavior was assessed (Fig. 2 A). The $t_{1/2}$ of occludin and ZO-1 increased in a nearly linear manner as monolayers were chilled from 37 to 14°C (Fig. 2 B). Interestingly, this paralleled transepithelial resistance (TER) increases (Fig. 2 B). In contrast, the occludin mobile fraction decreased only slightly between 37 and 17°C but was then sharply reduced at 14°C (Fig. 2 C), suggesting that membrane fluidity might be important to occludin FRAP behavior. The ZO-1 mobile fraction

Figure 2. **Occludin and ZO-1 FRAP are differentially dependent on membrane composition and metabolic energy.** (A) FRAP experiments were performed on monolayers of EGFP-occludin– and EGFP–ZO-1–expressing cells incubated at 37 (control), 18, or 14°C, with MBCD, or after ATP depletion. Representative kymographs are shown. (B and C) The $t_{1/2}$ and mobile fraction were calculated from FRAP experiments ($n \geq 5$ at each temperature). TER was measured in parallel. (D–F) TER and mobile fraction were determined in monolayers incubated with MBCD or after ATP depletion. $n \geq 5$ for each treatment. Error bars represent SEM. Bar, 2 µm.
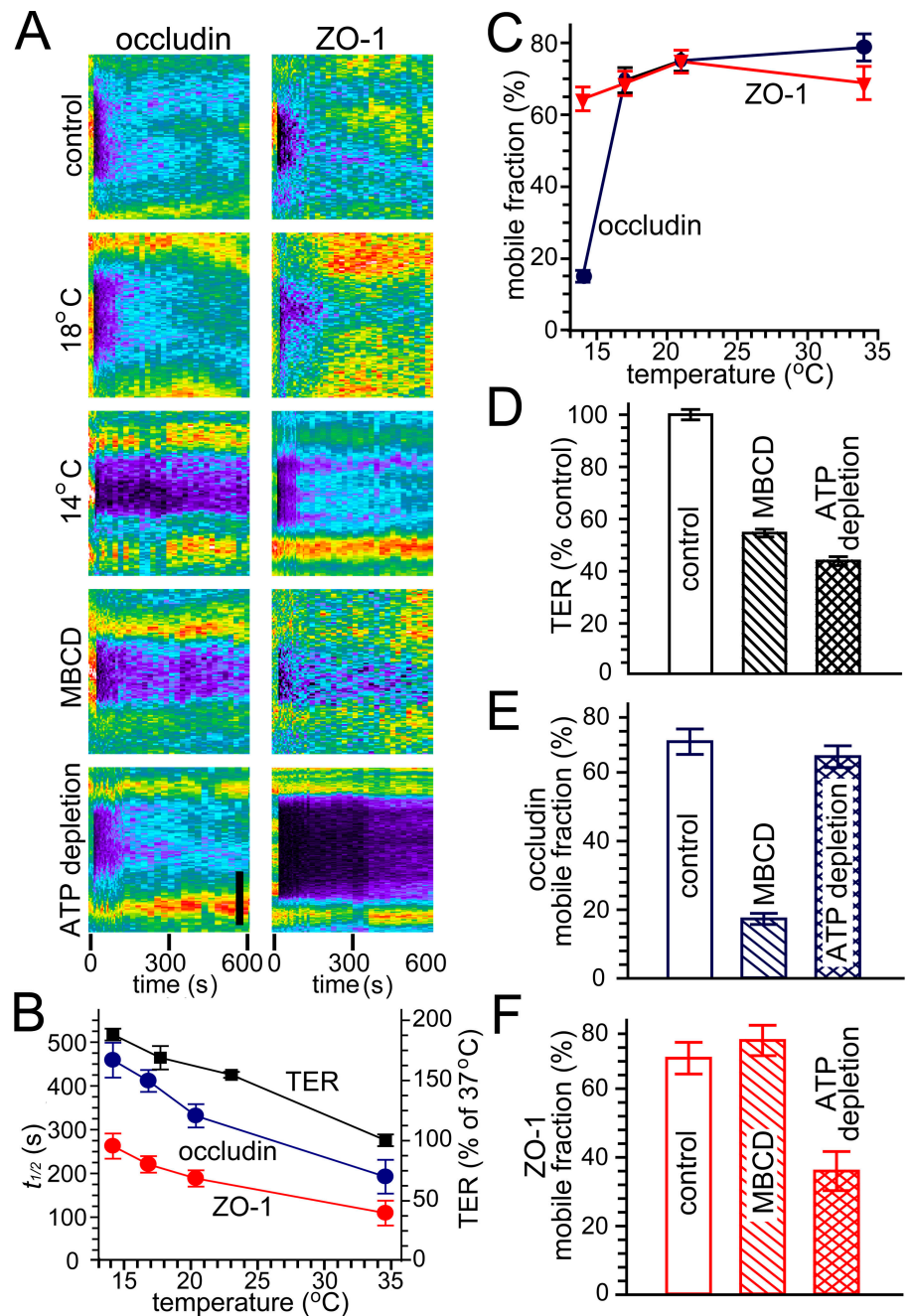
did not change significantly as monolayers were cooled from 37 to 14°C (Fig. 2 C).

Tight junction membranes are enriched in cholesterol, and cholesterol depletion is known to disrupt barrier function (Lynch et al., 1993; Francis et al., 1999). Thus, it is plausible that the observed decrease in occludin mobile fraction at 14°C is caused by the stabilization of cholesterol-rich tight junction membrane domains. To assess the effect of cholesterol depletion on occludin exchange, monolayers were treated with methyl-β-cyclodextrin (MBCD). This reduced TER by 45 ± 1% (Fig. 2 D) and also sharply reduced the occludin mobile fraction from 73 ± 4 to 18 ± 2% (P < 0.01; Fig. 2 E). In contrast, cholesterol depletion had no effect on ZO-1 FRAP behavior (Fig. 2 F). Because MBCD treatment affects both membrane fluidity and vesicular

traffic, these data suggest that occludin may recover by mechanisms that require these processes.

To further characterize the general mechanisms of occludin and ZO-1 exchange, FRAP behavior was assessed in metabolically depleted monolayers. Reduction of cellular ATP levels by 65 ± 5% had no effect on occludin FRAP dynamics, although TER decreased by 56 ± 2% (Fig. 2 D). In contrast, ATP depletion reduced the ZO-1 mobile fraction to 36 ± 6% (Fig. 2 F) and the β-actin mobile fraction to 19 ± 4% (not depicted). These findings show that occludin and ZO-1 dynamics require distinct factors. Furthermore, the differential regulation of occludin and ZO-1 dynamics by these treatments supports the conclusion that occludin and ZO-1 do not form stable complexes at the tight junction.
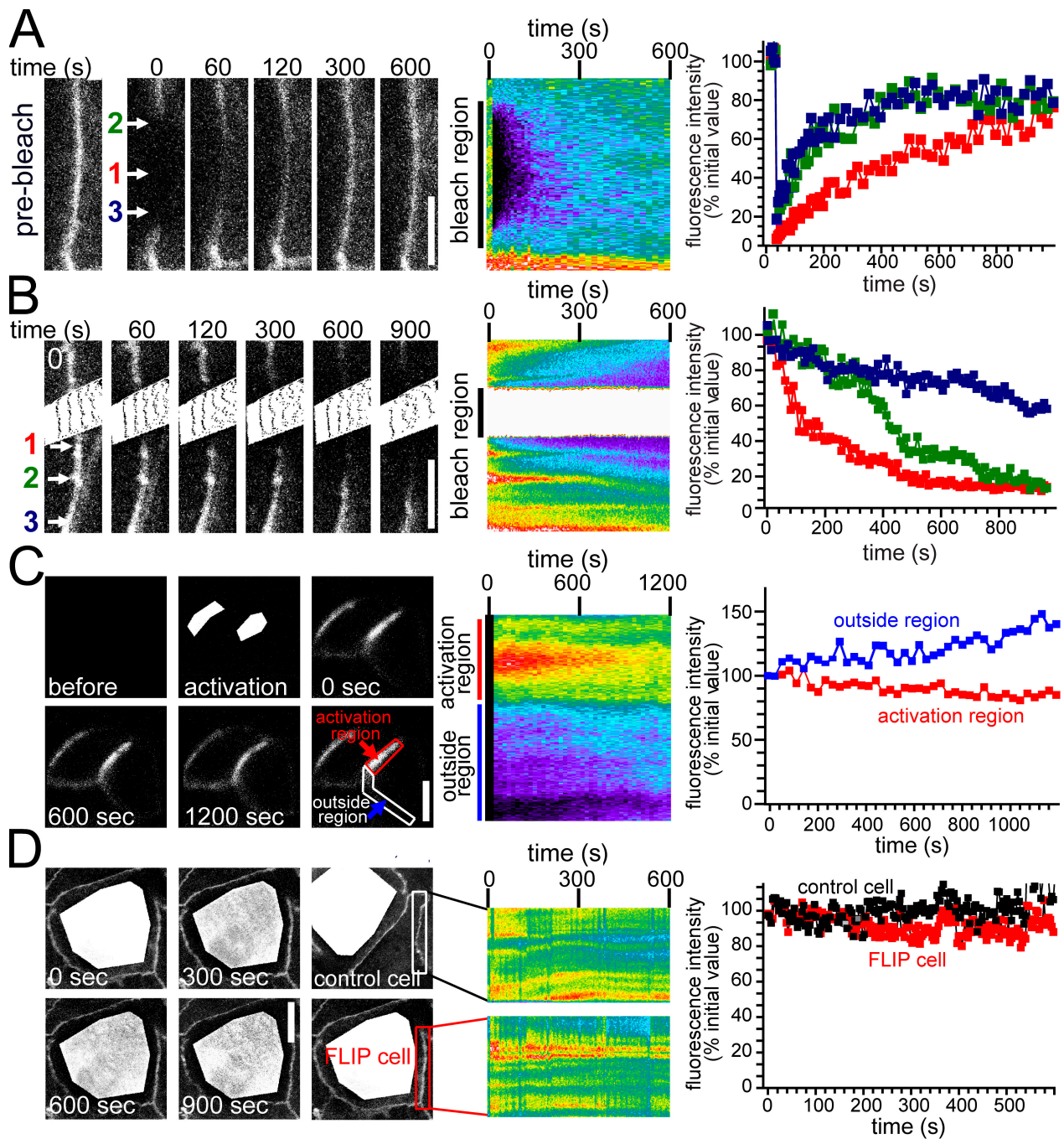
Figure 3. **Occludin diffuses within tight junction.** (A) EGFP-occludin–expressing cells within confluent monolayers were studied by FRAP after photobleaching elongated tight junction regions. Representative images before and at the indicated time points after photobleaching and the corresponding kymograph are shown. (B) The effect of continuous photobleaching of EGFP-occludin within a region of the tight junction is shown in representative images at the indicated times and in the corresponding kymograph. (A and B) Quantitative analysis of the individual sites indicated by the colored arrows is shown at the right. (C) Fluorescence of PA-GFP was activated in the white areas shown in the image collected during activation. Images collected at subsequent times show diffusion of activated PA-GFP–occludin to adjacent regions. The corresponding kymograph and quantitative analysis of the indicated activation region and adjacent region are shown. (D) The effect of continuous intracellular photobleaching of an EGFP-occludin–expressing cell within a confluent monolayer is shown. The kymographs and quantitative analyses show FLIP analysis of tight junction–associated EGFP-occludin within the indicated regions of photobleached and adjacent control cells. Bars: (A and B) 5 µm; (C and D) 10 µm.

The primary mechanism of occludin exchange is diffusion within the plasma membrane

Although fractions of the occludin and ZO-1 available for exchange are similar, the differences in $t_{1/2}$ and sensitivity to perturbations that alter membrane function or metabolic energy content suggest that distinct mechanisms are involved in the observed FRAP behaviors of these proteins. To preliminarily determine the mechanism of occludin recovery at the tight junction, an ∼10-µm segment of the tight junction was bleached,
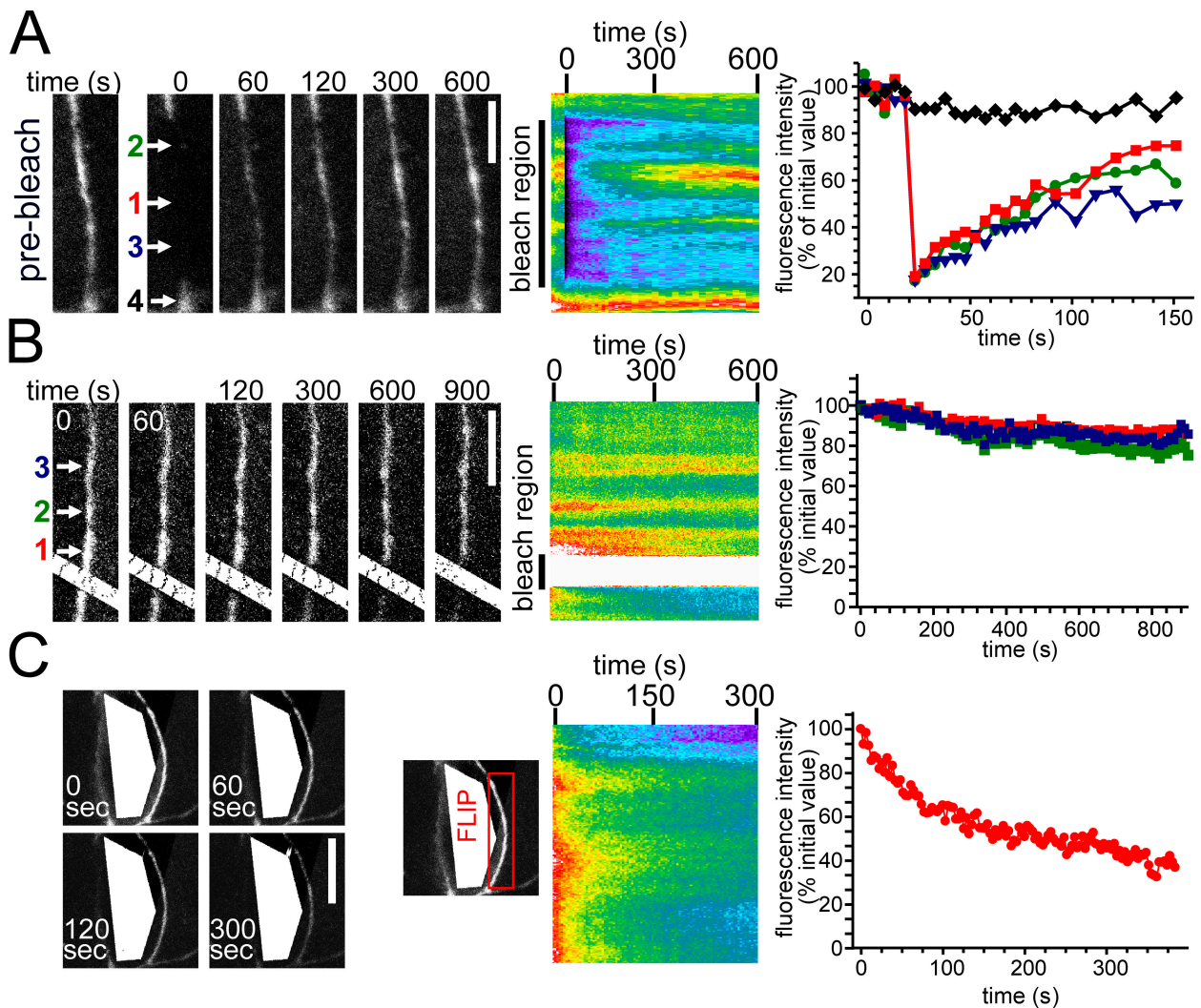
Figure 4. **Tight junction–associated ZO-1 exchanges with an intracellular pool.** (A) EGFP–ZO-1–expressing cells within confluent monolayers were studied by FRAP after photobleaching elongated tight junction regions. Representative images before and at the indicated times after photobleaching and the corresponding kymograph are shown. (B) The effect of continuous photobleaching of EGFP–ZO-1 within a region of the tight junction is shown in representative images at the indicated times and in the corresponding kymograph. (A and B) Quantitative analysis of the individual sites indicated by the colored arrows is shown at the right. (C) The effect of continuous intracellular photobleaching of an EGFP–ZO-1–expressing cell within a confluent monolayer is shown. The kymograph and quantitative analysis show tight junction–associated EGFP–ZO-1 fluorescence within the indicated tight junction region of a photobleached cell. Bars: (A and B) 5 µm; (C) 10 µm.

and recovery was monitored in the center and edges of this region. Fluorescent recovery began at the edges; the center of the bleached region recovered only after a lag of ∼500 s (Fig. 3 A). Because total occludin content within the tight junction is constant at steady state and fluorescent recovery represents the recruitment of unbleached occludin molecules into the bleached region, this suggests that occludin moves by diffusion within the membrane. Two separate approaches were used to directly assess occludin movement at steady state. First, the fluorescent loss in photobleaching (FLIP) technique was used to continuously bleach a small region of the tight junction. Consistent with occludin diffusion within the membrane, loss of fluorescence occurred most rapidly in areas directly adjacent to the bleached region, whereas fluorescence loss occurred more slowly at greater distances from the bleached region (Fig. 3 B). A complementary experiment made use of an occludin construct containing photo-activatable (PA) GFP (Patterson and Lippincott-Schwartz, 2002).

As shown in Fig. 3 C, occludin fluorescence was activated at two tight junction regions. Although total tight junction fluorescence remained constant after activation, occludin fluorescence decreased progressively in areas of activation and increased in adjacent regions of the tight junction, demonstrating occludin exchange between these areas (Fig. 3 C). These data confirm that a principal mode of occludin exchange is diffusion within the membrane.

The aforementioned experiments do not exclude a contribution of vesicular traffic to the observed occludin FRAP. This is critical, as occludin has frequently been reported in cytoplasmic vesicles, and endocytic removal of occludin from the tight junction correlates with barrier loss in response to a variety of stimuli (Furuse et al., 1996; Lapierre et al., 1999; Ye et al., 1999; Clayburgh et al., 2005; Shen and Turner, 2005; Schwarz et al., 2007). Intracellular occludin-containing vesicles are readily seen within transfected monolayers (Shen and Turner, 2005). However, fluorescent intracellular vesicles were not apparent after
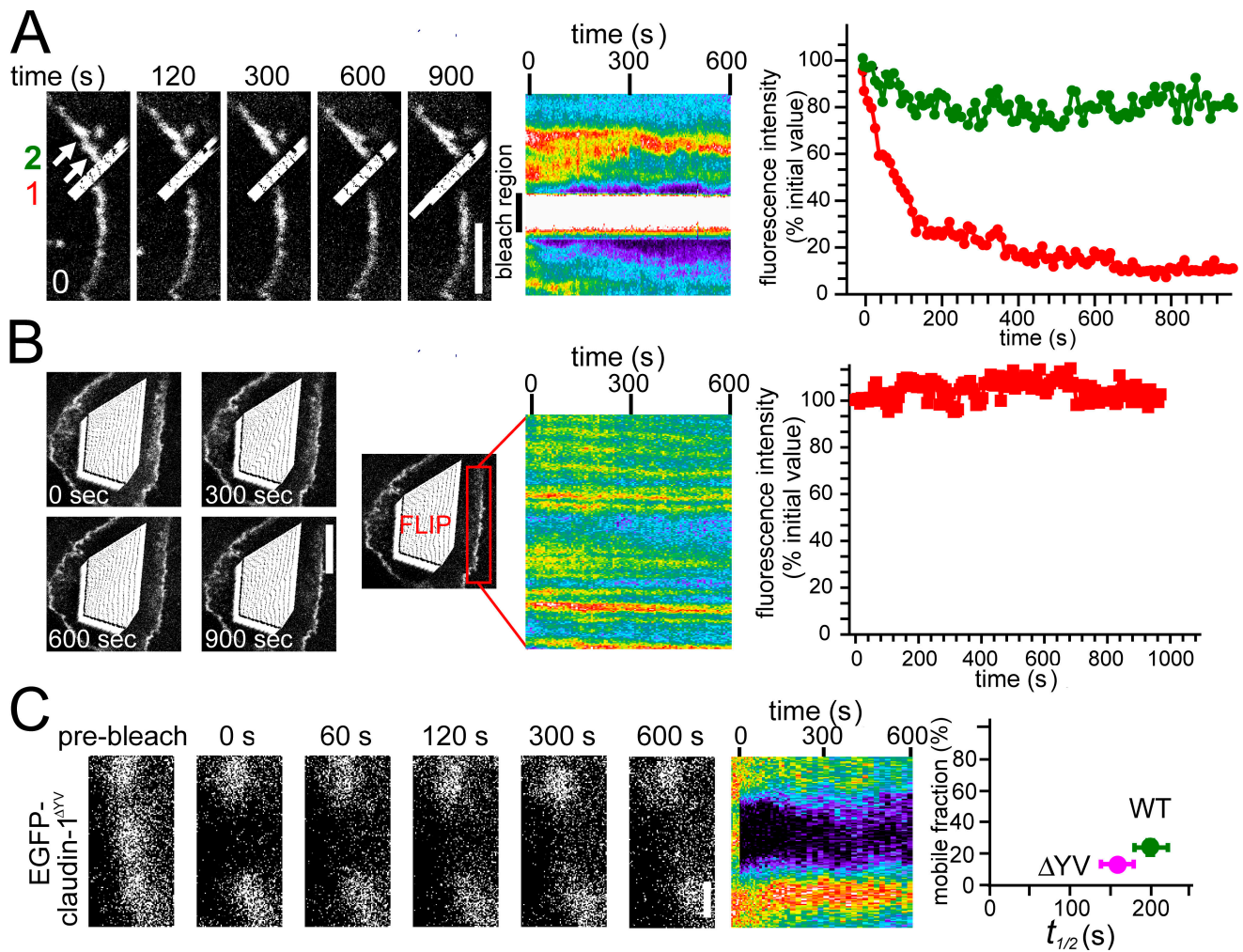
Figure 5.   **Limited claudin-1 exchange occurs by diffusion within the tight junction.** (A) EGFP–claudin-1–expressing cells within confluent monolayers were studied by continuous photobleaching of a region of the tight junction. Representative images at indicated times and the corresponding kymograph show the effect on tight junction fluorescence. Quantitative analysis of the individual sites indicated by the colored arrows is shown at the right. (B) The effect of continuous intracellular photobleaching of an EGFP–claudin-1–expressing cell within a confluent monolayer is shown. The kymograph and quantitative analysis shows tight junction–associated EGFP–claudin-1 fluorescence within the indicated region of a photobleached cell before and at intervals after photobleaching. (C) High magnification images and corresponding kymograph of EGFP–claudin-1$^{\Delta YV}$ are shown. The mobile fraction and $t_{1/2}$ of wild-type EGFP–claudin-1 and EGFP–claudin-1$^{\Delta YV}$ are shown in the graph at the right. Bars: (A) 5 µm; (B) 10 µm; (C) 2 µm.

activation of tight junction–associated PA-GFP–occludin (Fig. 3 C), suggesting that at steady state, large quantities of occludin do not routinely leave the tight junction to be concentrated in cytoplasmic vesicles. In addition, FLIP analysis showed that continuous photobleaching of the entire intracellular region, sparing the tight junction, only slightly diminished tight junction–associated occludin fluorescence (Fig. 3 D). Thus, the recognized intracellular pool of occludin does not exchange rapidly with tight junction–associated occludin at steady state. As an additional test of this conclusion, the guanine exchange factor inhibitor brefeldin A, which blocks multiple exocytic and endocytic processes, was applied to monolayers. Brefeldin A did not inhibit occludin FRAP at the tight junction (unpublished data), confirming that intracellular pools of occludin are not transported to the tight junction at rates sufficient to explain the observed occludin FRAP. However, brefeldin A treatment decreased epithelial barrier function progressively over 2 h, suggesting that membrane traffic may be important to the maintenance of tight junction integrity.

Collectively, these data show that the observed occludin FRAP behavior occurs primarily by diffusion within the membrane and that delivery of occludin from an intracellular pool participates either to a minor extent or not at all.

Tight junction–associated ZO-1 exchanges with an intracellular ZO-1 pool

As demonstrated in Fig. 1, although ZO-1 and occludin display similar mobile fractions at the tight junction, ZO-1 fluorescence recovers more rapidly than does occludin. Thus, experiments similar to those used to assess the mechanisms of occludin recovery were used to determine the mechanisms of ZO-1 recovery at the tight junction. In contrast to the results obtained with occludin, similar rates and extents of fluorescent recovery were seen at the center and edges after bleaching an extended ∼10-µm region of the tight junction (Fig. 4 A). In addition, FLIP analysis showed that continuous bleaching of a small region of the tight junction resulted in only limited fluorescence loss in adjacent and distant
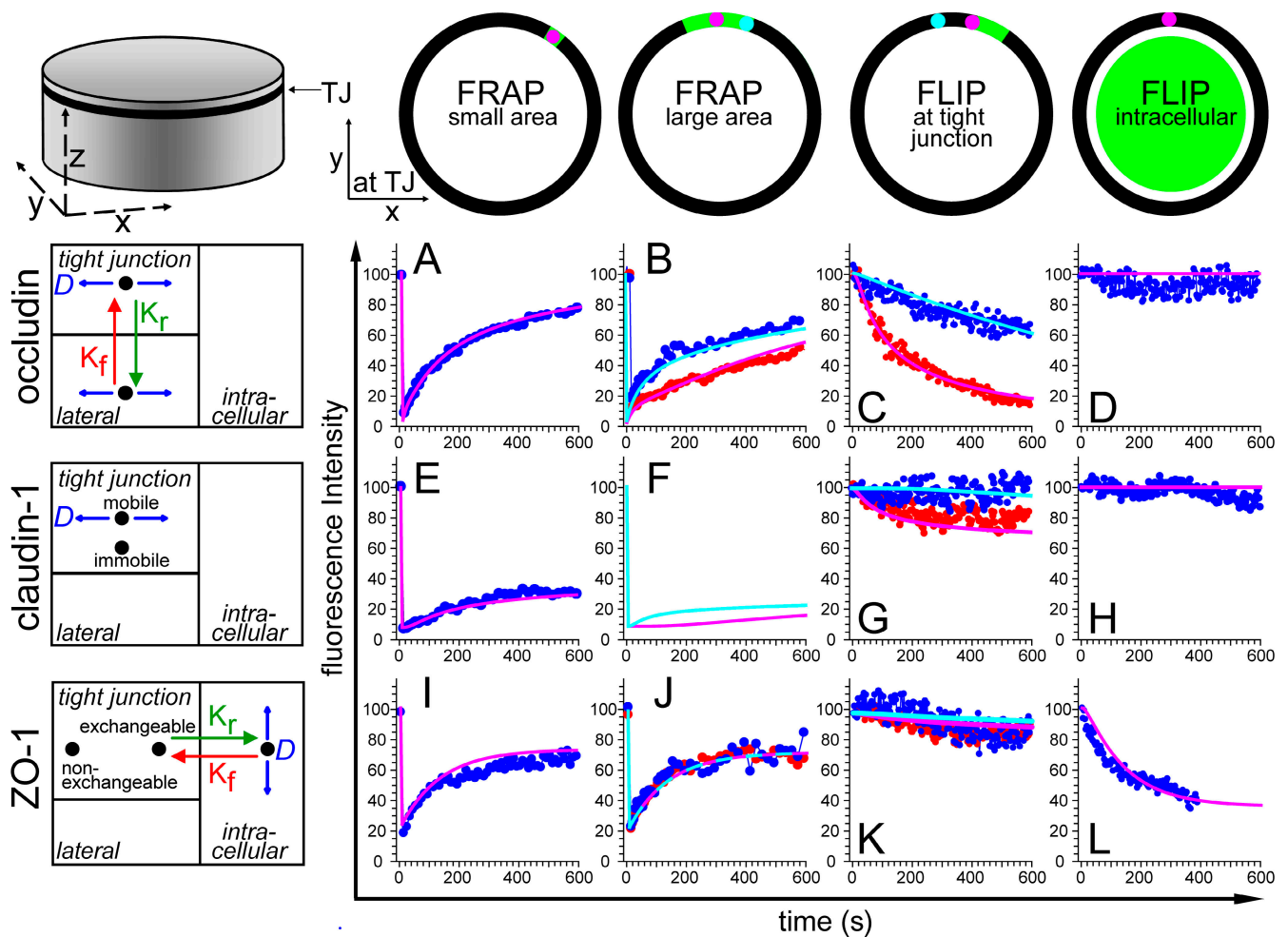
Figure 6. **In silico simulations accurately model tight junction protein dynamic behavior.** Computer models were established to predict tight junction protein dynamics (pink and cyan lines in A–L) and were compared with experimental data (red and blue symbols in A–L) for occludin (A–D), claudin-1 (E–H), and ZO-1 (I–L). Small area FRAP (A, E, and I), large area FRAP (B, F, and J), tight junction FLIP (C, G, and K), and intracellular FLIP experiments (D, H, and L) are compared. The models at the left show the assumptions required for the simulation to fit the experimental data. Specific values are given in Table II.

regions of the tight junction (Fig. 4 B). These data suggest that ZO-1 does not recover by diffusion within the membrane but by exchange with a separate pool. This was unexpected, as it is difficult to detect intracellular ZO-1 pools immunohistochemically. Although some nuclear EGFP–ZO-1 is present in subconfluent monolayers, which is consistent with a study of nuclear ZO-1 in undifferentiated epithelia (Gottardi et al., 1996), only faint intracellular fluorescence is detectable in cells expressing EGFP–ZO-1. FLIP analysis with continuous intracellular bleaching was used to evaluate the presence or absence of intracellular ZO-1 pools. This maneuver resulted in progressive decreases in tight junction–associated ZO-1 fluorescence (Fig. 4 C). As these experiments were performed only on confluent monolayers where no nuclear ZO-1 is detected, the intracellular pool of ZO-1 is likely cytoplasmic. Tight junction–associated ZO-1 fluorescent loss measured by FLIP occurs with a $t_{1/2}$ of 89 ± 17 s, similar to the $t_{1/2}$ of 119 ± 21 s for exchange measured by FRAP. Therefore, these data demonstrate that a large fraction of tight junction–associated ZO-1 exchanges continuously with an intracellular pool. These studies also show that a small nonexchangeable pool of ZO-1 exists at the tight junction. The interactions that anchor this subset

of ZO-1 at the tight junction are not defined, but this non-exchangeable pool increases between 1 and 3 d after confluence (Table I), suggesting that anchoring is related to the process of tight junction maturation.

Claudin-1 exchange occurs by limited diffusion within the tight junction

In contrast to occludin and ZO-1, claudin-1 exhibits little fluorescent recovery. To assess the mechanisms of claudin-1 exchange, FLIP experiments similar to those described for occludin and ZO-1 were performed. Continuous bleaching of a small region of the tight junction showed rapid loss of claudin-1 fluorescence in the immediately adjacent area but not at more distant regions (Fig. 5 A). This is consistent with the limited mobile fraction observed in the initial claudin-1 FRAP experiments and suggests that claudin-1 also exchanges by diffusion within the tight junction. Continuous intracellular photobleaching had no significant effect on tight junction–associated claudin-1 fluorescence (Fig. 5 B), suggesting that exchange between the tight junction and intracellular claudin-1 pools is minimal during the interval of these experiments.

Table II. **Parameters that define tight junction protein dynamic behavior in computer simulations**

Tight junction protein	Value
Occludin	
Tight junction fraction (all mobile)	80%
Lateral membrane fraction (all mobile)	20%
Intracellular fraction	0%
Tight junction diffusion constant	0.011 $\mu m^2 s^{-1}$
Lateral membrane diffusion constant	0.1 $\mu m^2 s^{-1}$
Rate constant for movement to tight junction (K_f)	0.0040 s^{-1}
Rate constant for movement from tight junction (K_r)	0.0010 s^{-1}
Claudin-1	
Tight junction fraction	100%
Immobile fraction at the tight junction	60%
Mobile fraction at the tight junction	40%
Lateral membrane fraction	0%
Intracellular fraction	0%
Tight junction diffusion constant, immobile fraction	0 $\mu m^2 s^{-1}$
Tight junction diffusion constant, mobile fraction	0.011 $\mu m^2 s^{-1}$
ZO-1	
Tight junction fraction	40%
Exchangeable fraction at the tight junction	25%
Nonexchangeable fraction at the tight junction	15%
Lateral membrane fraction	0%
Intracellular fraction	60%
Tight junction diffusion constant, exchangeable and nonexchangeable fractions	0 $\mu m^2 s^{-1}$
Intracellular diffusion constant	1 $\mu m^2 s^{-1}$
Rate constant for movement to tight junction (K_f), exchangeable fraction	0.25 $\mu m^2 s^{-1}$
Rate constant for movement from tight junction (K_r), exchangeable fraction	0.0075 s^{-1}
Rate constant for movement to tight junction (K_f), nonexchangeable fraction	0 $\mu m^2 s^{-1}$
Rate constant for movement from tight junction (K_r), nonexchangeable fraction	0 s^{-1}

The aforementioned data demonstrate that the majority of claudin-1 is immobile at the tight junction. Although the majority of ZO-1 at the tight junction is exchangeable, the mobile fraction is ∼70% in monolayers with fully assembled tight junctions (Table I), suggesting that a small but significant fraction of tight junction–associated ZO-1 is nonexchangeable. Therefore, it is possible that the immobile pool of tight junction–associated claudin-1 is anchored by binding to nonexchangeable ZO-1 molecules. To explore this possibility, an EGFP–claudin-1 mutant lacking the C-terminal YV motif necessary for PDZ binding was expressed in MDCK cells. Although trafficking of EGFP–claudin-1$^{\Delta YV}$ to the tight junction is defective, localization to cell contact sites does occur in some cells. Remarkably, tight junction–associated EGFP–claudin-1$^{\Delta YV}$ displayed a mobile fraction of 13 ± 2%, which is significantly lower than that of wild-type EGFP–claudin-1 (P < 0.05). The $t_{1/2}$ of EGFP–claudin-1$^{\Delta YV}$ was similar to that of wild-type EGFP–claudin-1 (Fig. 5 C). Thus, although it is clear that the PDZ-binding motif of claudin-1 is important for initial delivery, these data suggest that interactions requiring the C-terminus YV are not necessary for anchoring the majority of claudin-1 at the tight junction.

Quantitative modeling of tight junction protein exchange processes

To test the qualitative conclusions developed above and mathematically model tight junction protein exchange, MDCK cells were simulated as cylinders. Based on their observed distributions,

occludin, claudin-1, and ZO-1 were distributed among the lateral membrane, tight junction, and intracellular compartments (Table II). The mobility of each protein was defined based on the physical data shown in Figs. 1–4. Small area FRAP, large area FRAP, tight junction FLIP, and intracellular FLIP were performed by varying location, duration, and intensity of the virtual laser pulse without altering mobility parameters for each protein (Fig. 6).

To test whether simple diffusion within the tight junction is sufficient to account for the observed occludin behavior in FRAP and FLIP experiments, a model was developed with occludin localized only at the tight junction (unpublished data). In small area FRAP experiments (∼3 µm), 89% of observed occludin recovery at 600 s could be explained using simple diffusion within the tight junction and a diffusion constant of 0.011 $\mu m^2 s^{-1}$ (Table II). However, this simulation did not accurately model larger area FRAP and tight junction–bleaching FLIP experiments. To improve the simulation, a lateral membrane pool of occludin was included. This pool was modeled to represent 20% of total cellular occludin and was allowed to exchange with tight junction–associated occludin according to the following equation: $J_{occ} = (K_{f\,occ} \times [occ]_{lat}) - (K_{r\,occ} \times [occ]_{TJ})$. Using the determined rate constants (Table II), this simulation accurately modeled recovery within large and small photobleached areas (Fig. 6, A and B). Including lateral membrane occludin in the model also allowed accurate simulation of FLIP experiments in which a region of the tight junction was bleached

continuously (Fig. 6 C). Although it is clear from imaging experiments that an intracellular pool of occludin is frequently present, it was not necessary to include this component in the models, which is consistent with the conclusion that intracellular occludin pools do not contribute significantly to the observed FRAP and FLIP behaviors. This is confirmed by FLIP with continuous intracellular bleaching (Fig. 6 D). In contrast, the exchange of lateral membrane– and tight junction–associated occludin is necessary for the simulations to accurately model the physical observations, suggesting that this exchange does contribute to FRAP and FLIP behaviors and that lateral membrane occludin may diffuse more rapidly than tight junction occludin. An immobile fraction is not necessary for the accurate modeling of occludin dynamic behavior, suggesting that the observed immobile fraction may reflect technical limitations rather than physical retention.

The $t_{1/2}$ of claudin-1 recovery in small area FRAP experiments was similar to that of occludin (Fig. 1). Thus, claudin-1 exchange was modeled with a diffusion constant of 0.011 $\mu m^2 s^{-1}$, which is identical to that used for occludin. An immobile fraction representing 60% of total claudin-1 was included to model the large immobile fraction observed experimentally. This model accurately simulates small (Fig. 6 E) and large (Fig. 6 F) area FRAP experiments. As an alternative to a large claudin-1 immobile fraction, models in which the diffusion constant for claudin-1 was reduced were developed. These were able to display recovery at 600 s but did not accurately represent the experimentally determined $t_{1/2}$ of claudin-1 recovery. Moreover, the model including a large claudin-1 immobile fraction accurately simulated FLIP experiments bleaching tight junction (Fig. 6 G) and intracellular regions (Fig. 6 H). Thus, the simulation suggests that tight junction–associated claudin-1 and occludin recover by diffusion within the membrane at similar rates. However, in contrast to occludin, claudin-1 has a prominent immobile fraction.

As suggested by the physical data, ZO-1 could not be modeled by simple diffusion within membrane compartments. The physical observations that prevented such modeling were that (1) recovery within different parts of photobleached areas occurred uniformly; (2) overall recovery rates after bleaching large and small areas were identical; and (3) tight junction–associated ZO-1 fluorescence decreased after continuous intracellular photobleaching. To model the dynamic behavior of ZO-1, the exchange between tight junction and intracellular pools was allowed to occur as described by the following equation: $J_{ZO-1} = (K_{f\,ZO-1} \times [ZO\text{-}1]_{cyt}) - (K_{r\,ZO-1} \times [ZO\text{-}1]_{TJ})$. This required 60% of ZO-1 to be cytosolic, with the remaining 40% localized to the tight junction and divided into exchangeable and nonexchangeable pools (Table II). This model accurately simulated small (Fig. 6 I) and large (Fig. 6 J) area FRAP experiments. The model also predicts the observed small 9% decay in regions adjacent to the photobleached region in FLIP experiments (Fig. 6 K) as well as the large decreases in tight junction fluorescence seen in intracellular FLIP experiments (Fig. 6 L). Therefore, this model accurately simulates all observed ZO-1 behavior on the basis of exchange between tight junction and intracellular pools without any diffusion within the

tight junction. Notably, a nonexchangeable pool at the tight junction is required to accurately model ZO-1 behavior.

Discussion

The explosion in recognized tight junction–associated proteins and identification of interactions between these proteins has led to the widespread agreement that the tight junction is a complex of multiple cross-linked proteins (Tsukita et al., 2001; Peng et al., 2003; Anderson et al., 2004). This has led to the development of a model in which assembled tight junctions in intact steady-state epithelia are static and is consistent with observations of stable structure and barrier function over time.

However, relatively little direct evidence supports this view. For example, behavior of fluorescent-tagged claudin proteins has been studied to only a limited degree in epithelial cells and fibroblasts. In the latter, which do not form tight junctions, claudin proteins assemble into long fibrils within the plasma membrane (Sasaki et al., 2003). Although these strands interact with one another and frequently move within the plasma membrane, FRAP analysis showed that claudin-1 within these strands is immobile (Sasaki et al., 2003). This observation lent support to the belief that proteins within the tight junction are immobile or static.

The data presented here directly contradict the static model of tight junction structure. One piece of evidence supporting this conclusion is that each of the tight junction–associated proteins studied displays distinct dynamic behaviors and mechanisms of exchange. Approximately 70% of tight junction–associated ZO-1 and occludin are each present within the mobile fraction. This might imply that they traffic as a complex. However, subsequent investigation demonstrated that the rates and mechanisms of exchange differ for these proteins. Therefore, they do not exchange in complex with one another. Although only 24% of claudin-1 is in the mobile fraction, a number far greater than that suggested by experiments in fibroblasts, it should be noted that this also indicates that the majority of tight junction–associated claudin-1 resides within an immobile pool. The interactions that anchor claudin-1 at the tight junction remain to be determined, but the experiments using claudin-1$^{\Delta YV}$ suggest that stable binding between claudin-1 and PDZ domains of ZO-1, -2, and other tight junction proteins are not required. In fact, interaction between the claudin-1 C terminus and PDZ domains may promote claudin-1 exchange within the tight junction, as claudin-1$^{\Delta YV}$ has a smaller mobile fraction than wild-type claudin-1. Consistent with the conclusion that interactions with endogenous full-length claudin or other proteins stabilizes EGFP–claudin-1$^{\Delta YV}$ at the tight junction, a previous study has shown that claudin-1–EGFP, in which EGFP placement at the C terminus obstructs interactions with ZO-1, displays limited exchange within the tight junction–like strands that develop in fibroblasts (Sasaki et al., 2003). Nonetheless, interactions between the claudin-1 C terminus and PDZ domains are important in directing claudin-1 to localize at the tight junction, as claudin-1$^{\Delta YV}$ protein trafficking to cell contact sites was clearly defective.

The data clearly demonstrate that the majority of tight junction–associated ZO-1, occludin, claudin-1, and β-actin do

not remain bound to one another at steady state. How can a model of tight junction structure be developed to accommodate these new data? One point that must be considered is that 31% of tight junction–associated ZO-1 does not exchange over the course of these FRAP and FLIP experiments. Together with the mathematical modeling of ZO-1 behavior, which required the inclusion of a nonexchangeable pool to accurately simulate the physical data, these data suggest that a stable pool of ZO-1 exists at the tight junction. Although the functional differences between exchangeable and nonexchangeable ZO-1 and the relevance of these pools to tight junction function remain to be determined, the studies of general perturbations, including temperature modulation, cholesterol chelation, and ATP depletion, make it clear that any relationships between FRAP behavior and barrier function must be complex and dependent on many factors. Similar questions may be asked about occludin diffusion within the tight junction membrane, although controversy remains regarding the function of this protein (Furuse et al., 1993; Chen et al., 1997; Sakakibara et al., 1997; Van Itallie and Anderson, 1997; Wong and Gumbiner, 1997; Li and Mrsny, 2000; Saitou et al., 2000; Kuwabara et al., 2001; Schulzke et al., 2005; Yu et al., 2005). It is also likely that the constant movement of proteins within the tight junction and the observed exchange of these proteins with extra-tight junction pools are important to the rapid structural and functional responses to stimuli. In the absence of such plasticity, it is perhaps hard to understand how barrier function can be modified in minutes.

In conclusion, the data presented here show that each of the proteins studied is surprisingly dynamic at the tight junction and that these dynamics are kinetically distinct as a result of different mechanisms of exchange. These results demand that the prevailing model of tight junction structure be revised to incorporate the idea that interactions between tight junction proteins are transient and characterized by continuous engagement and release. Future characterization of the structural domains and elements that control the dynamic behaviors of tight junction proteins promises to finally provide molecular characterization of tight junction regulation.

Materials and methods

Plasmids
EGFP–β-actin and EGFP–claudin-1 constructs were generated as reported previously (Shen and Turner, 2005). EGFP–claudin-1$^{\Delta YV}$ was created by site-directed mutagenesis to create a premature stop codon (Stratagene). EGFP- and PA-GFP–tagged occludin were generated by PCR amplification and cloning of the coding region of human occludin (a gift from R.J. Mrsny, Cardiff University, Cardiff, UK) into KpnI–XbaI sites of pEGFP-C1 (Clontech Laboratories, Inc.) and PA-GFP (a gift from J. Lippincott-Schwartz, National Institute of Child Health and Human Development, National Institutes of Health, Bethesda, MD) vectors in frame with EGFP or PA-GFP. EGFP–ZO-1 was generated by first inserting KpnI sites flanking the coding region of human ZO-1 (a gift from J. Anderson and A. Fanning, University of North Carolina at Chapel Hill, Chapel Hill, NC) and then cloning the coding region into the KpnI site of pEGFP-C1 in frame with EGFP. The integrity of all plasmids was verified by restriction digestion and direct sequencing.

FRAP and FLIP
MDCK cells were transfected and maintained as described previously (Shen and Turner, 2005) and were studied 3 d after confluence, except where otherwise indicated. Monolayers were transferred to bicarbonate-free HBSS supplemented with 15 mM Hepes, pH 7.4, at 37°C and mounted on a custom-designed temperature-controlled stage (Brook Industries) at 37°C for 30 min to allow equilibration. Confocal scanning light microscopy was performed by using a microscope system (TCS SP2 AOBS; Leica) with a 63× NA 1.40 oil immersion objective and a pinhole between 1 and 2 AU. EGFP fusion proteins were excited using the argon 488-nm laser line and emission gated between 490 and 530 nm. FRAP experiments were performed using the FRAP module of confocal software (Leica). A region of interest to be bleached was defined, and maximum laser power at the appropriate wavelength for an empirically determined number of iterations was used to bleach signals. Bleaching time was usually <10 s, resulting in bleaching throughout the full thickness of the tight junction. After bleaching, images were taken within the same focal plane at regular intervals (between 2 and 30 s) to monitor fluorescence recovery.

To test the continuity of different cellular pools of tight junction proteins, FLIP experiments were performed using the FLIP module of the confocal software. Observation and photobleaching were performed in the same scan for different regions of the scanning field. Continuous scanning was performed with no delay between scans for 5–15 min. For tight junction bleaching, a small area at the tight junction was continuously bleached at full laser power. For intracellular bleaching, a large area that encompasses ∼80% of the intracellular area at the tight junction level was continuously bleached at full laser power. In either case, the remainder of the field was observed using the laser at ∼10% power.

For inhibitor experiments, monolayers were treated with appropriate drugs in HBSS for 1 h before use. ATP depletion experiments were performed using glucose-free HBSS containing 2 mM 2-D-deoxy-glucose, 1 mM 2,4-dinitrophenol, and 10 mM NaN_3 to inhibit ATP generation. MBCD was used at 5 mM.

Fluorescence quantification and data analysis
Time series of image files were opened and converted to multipage image files using Image J (National Institutes of Health). Image analyses were performed by using MetaMorph 7 (MDS Analytical Technologies). Regions of interest were drawn, and the mean fluorescence intensity of each region was logged for each time point. For small area FRAP experiments, regions of interest were drawn at the center of the bleach region, which occupies a fraction of the whole bleaching area.

For all FRAP experiments, mean fluorescence in bleached areas was corrected for observation bleaching using a distant area of the tight junction for reference. The corrected data were fit to the equation below, which assumes that recovery involves a single coefficient (Yguerabide et al., 1982):

$$I(t) = \frac{I_0 + I_{max} \times t / t_{1/2}}{1 + t / t_{1/2}}.$$

Preliminary analyses showed that higher order equations did not improve the quality of fit. Using experimental data, the value for $t_{1/2}$ was calculated with nonlinear regression without any constraints using Sigma Plot (SPSS, Inc.). Mobile fraction was determined as

$$M_f = \frac{I_{max} - I_0}{1 - I_0}.$$

Computer simulation
A three-dimensional computer simulation was created to model the results of FRAP and FLIP experiments using the Virtual Cell biological modeling framework (www.vcell.org). Cells were modeled as cylinders with a diameter of 30 μm and a height of 10 μm to approximate the measured physical dimensions of MDCK cells in confluent monolayers. The tight junction was modeled as a 1-μm thick band. The model includes separate tight junction and extra tight junction membrane domains and an intracellular pool. A spatially defined laser was used to rapidly bleach 90% of fluorescent molecules within 1 s, and molecules diffused according to defined rate constants and spatial constraints. Simulations used 10-ms time steps with a spatial simulation mesh of 1 μm in the z axis and 0.6 μm in the xy axis. Fluorescent intensities were normalized to initial conditions. After assignment of different constants and restraints, only the location, duration, and intensity of the laser pulse were altered to simulate the various FRAP and FLIP experiments for each protein. The models used and data obtained can be accessed at http://vcell.org/applications/published%20models.html.

TER measurements
MDCK cells were plated at confluent density on semipermeable supports (Corning). TER was measured after 3 d using electrodes with a voltohmeter (EVOM; World Precision Instruments).

References

Anderson, J.M., C.M. Van Itallie, and A.S. Fanning. 2004. Setting up a selective barrier at the apical junction complex. *Curr. Opin. Cell Biol.* 16:140–145.

Balda, M.S., J.M. Anderson, and K. Matter. 1996. The SH3 domain of the tight junction protein ZO-1 binds to a serine protein kinase that phosphorylates a region C-terminal to this domain. *FEBS Lett.* 399:326–332.

Bazzoni, G., O.M. Martinez-Estrada, F. Orsenigo, M. Cordenonsi, S. Citi, and E. Dejana. 2000. Interaction of junctional adhesion molecule with the tight junction components ZO-1, cingulin, and occludin. *J. Biol. Chem.* 275:20520–20526.

Beatch, M., L.A. Jesaitis, W.J. Gallin, D.A. Goodenough, and B.R. Stevenson. 1996. The tight junction protein ZO-2 contains three PDZ (PSD-95/Discs-Large/ZO-1) domains and an alternatively spliced region. *J. Biol. Chem.* 271:25723–25726.

Bezprozvanny, I., and A. Maximov. 2001. PDZ domains: more than just a glue. *Proc. Natl. Acad. Sci. USA.* 98:787–789.

Carlton, V.E., B.Z. Harris, E.G. Puffenberger, A.K. Batta, A.S. Knisely, D.L. Robinson, K.A. Strauss, B.L. Shneider, W.A. Lim, G. Salen, et al. 2003. Complex inheritance of familial hypercholanemia with associated mutations in TJP2 and BAAT. *Nat. Genet.* 34:91–96.

Chen, Y.H., and Q. Lu. 2003. Association of nonreceptor tyrosine kinase c-yes with tight junction protein occludin by coimmunoprecipitation assay. *Methods Mol. Biol.* 218:127–132.

Chen, Y., C. Merzdorf, D.L. Paul, and D.A. Goodenough. 1997. COOH terminus of occludin is required for tight junction barrier function in early *Xenopus* embryos. *J. Cell Biol.* 138:891–899.

Citi, S., H. Sabanay, R. Jakes, B. Geiger, and J. Kendrick-Jones. 1988. Cingulin, a new peripheral component of tight junctions. *Nature.* 333:272–275.

Claude, P., and D.A. Goodenough. 1973. Fracture faces of zonulae occludentes from "tight" and "leaky" epithelia. *J. Cell Biol.* 58:390–400.

Clayburgh, D.R., T.A. Barrett, Y. Tang, J.B. Meddings, L.J. Van Eldik, D.M. Watterson, L.L. Clarke, R.J. Mrsny, and J.R. Turner. 2005. Epithelial myosin light chain kinase-dependent barrier dysfunction mediates T cell activation-induced diarrhea in vivo. *J. Clin. Invest.* 115:2702–2715.

Cordenonsi, M., F. D'Atri, E. Hammar, D.A. Parry, J. Kendrick-Jones, D. Shore, and S. Citi. 1999. Cingulin contains globular and coiled-coil domains and interacts with ZO-1, ZO-2, ZO-3, and myosin. *J. Cell Biol.* 147:1569–1582.

Dodane, V., and B. Kachar. 1996. Identification of isoforms of G proteins and PKC that colocalize with tight junctions. *J. Membr. Biol.* 149:199–209.

Ebnet, K., C.U. Schulz, M.K. Meyer Zu Brickwedde, G.G. Pendl, and D. Vestweber. 2000. Junctional adhesion molecule interacts with the PDZ domain-containing proteins AF-6 and ZO-1. *J. Biol. Chem.* 275:27979–27988.

Fanning, A.S., B.J. Jameson, L.A. Jesaitis, and J.M. Anderson. 1998. The tight junction protein ZO-1 establishes a link between the transmembrane protein occludin and the actin cytoskeleton. *J. Biol. Chem.* 273:29745–29753.

Fanning, A.S., T.Y. Ma, and J.M. Anderson. 2002. Isolation and functional characterization of the actin binding region in the tight junction protein ZO-1. *FASEB J.* 16:1835–1837.

Fanning, A.S., B.P. Little, C. Rahner, D. Utepbergenov, Z. Walther, and J.M. Anderson. 2007. The unique-5 and -6 motifs of ZO-1 regulate tight junction strand localization and scaffolding properties. *Mol. Biol. Cell.* 18:721–731.

Farquhar, M.G., and G.E. Palade. 1963. Junctional complexes in various epithelia. *J. Cell Biol.* 17:375–412.

Francis, S.A., J.M. Kelly, J. McCormack, R.A. Rogers, J. Lai, E.E. Schneeberger, and R.D. Lynch. 1999. Rapid reduction of MDCK cell cholesterol by methyl-beta-cyclodextrin alters steady state transepithelial electrical resistance. *Eur. J. Cell Biol.* 78:473–484.

Furuse, M., T. Hirase, M. Itoh, A. Nagafuchi, S. Yonemura, S. Tsukita, and S. Tsukita. 1993. Occludin: a novel integral membrane protein localizing at tight junctions. *J. Cell Biol.* 123:1777–1788.

Furuse, M., M. Itoh, T. Hirase, A. Nagafuchi, S. Yonemura, and S. Tsukita. 1994. Direct association of occludin with ZO-1 and its possible involvement in the localization of occludin at tight junctions. *J. Cell Biol.* 127:1617–1626.

Furuse, M., K. Fujimoto, N. Sato, T. Hirase, and S. Tsukita. 1996. Overexpression of occludin, a tight junction-associated integral membrane protein, induces the formation of intracellular multilamellar bodies bearing tight junction-like structures. *J. Cell Sci.* 109:429–435.

Furuse, M., K. Fujita, T. Hiiragi, K. Fujimoto, and S. Tsukita. 1998. Claudin-1 and -2: novel integral membrane proteins localizing at tight junctions with no sequence similarity to occludin. *J. Cell Biol.* 141:1539–1550.

Gonzalez-Mariscal, L., A. Betanzos, and A. Avila-Flores. 2000. MAGUK proteins: structure and role in the tight junction. *Semin. Cell Dev. Biol.* 11:315–324.

Gottardi, C.J., M. Arpin, A.S. Fanning, and D. Louvard. 1996. The junction-associated protein, zonula occludens-1, localizes to the nucleus before the maturation and during the remodeling of cell-cell contacts. *Proc. Natl. Acad. Sci. USA.* 93:10779–10784.

Hamazaki, Y., M. Itoh, H. Sasaki, M. Furuse, and S. Tsukita. 2002. Multi-PDZ domain protein 1 (MUPP1) is concentrated at tight junctions through its possible interaction with claudin-1 and junctional adhesion molecule. *J. Biol. Chem.* 277:455–461.

Haskins, J., L. Gu, E.S. Wittchen, J. Hibbard, and B.R. Stevenson. 1998. ZO-3, a novel member of the MAGUK protein family found at the tight junction, interacts with ZO-1 and occludin. *J. Cell Biol.* 141:199–208.

Hurd, T.W., L. Gao, M.H. Roh, I.G. Macara, and B. Margolis. 2003. Direct interaction of two polarity complexes implicated in epithelial tight junction assembly. *Nat. Cell Biol.* 5:137–142.

Ikenouchi, J., M. Furuse, K. Furuse, H. Sasaki, and S. Tsukita. 2005. Tricellulin constitutes a novel barrier at tricellular contacts of epithelial cells. *J. Cell Biol.* 171:939–945.

Itoh, M., A. Nagafuchi, S. Yonemura, T. Kitani-Yasuda, and S. Tsukita. 1993. The 220-kD protein colocalizing with cadherins in non-epithelial cells is identical to ZO-1, a tight junction-associated protein in epithelial cells: cDNA cloning and immunoelectron microscopy. *J. Cell Biol.* 121:491–502.

Itoh, M., A. Nagafuchi, S. Moroi, and S. Tsukita. 1997. Involvement of ZO-1 in cadherin-based cell adhesion through its direct binding to alpha catenin and actin filaments. *J. Cell Biol.* 138:181–192.

Itoh, M., M. Furuse, K. Morita, K. Kubota, M. Saitou, and S. Tsukita. 1999. Direct binding of three tight junction-associated MAGUKs, ZO-1, ZO-2, and ZO-3, with the COOH termini of claudins. *J. Cell Biol.* 147:1351–1363.

Izumi, Y., T. Hirose, Y. Tamai, S. Hirai, Y. Nagashima, T. Fujimoto, Y. Tabuse, K.J. Kemphues, and S. Ohno. 1998. An atypical PKC directly associates and colocalizes at the epithelial tight junction with ASIP, a mammalian homologue of *Caenorhabditis elegans* polarity protein PAR-3. *J. Cell Biol.* 143:95–106.

Jesaitis, L.A., and D.A. Goodenough. 1994. Molecular characterization and tissue distribution of ZO-2, a tight junction protein homologous to ZO-1 and the *Drosophila* discs-large tumor suppressor protein. *J. Cell Biol.* 124:949–961.

Kale, G., A.P. Naren, P. Sheth, and R.K. Rao. 2003. Tyrosine phosphorylation of occludin attenuates its interactions with ZO-1, ZO-2, and ZO-3. *Biochem. Biophys. Res. Commun.* 302:324–329.

Kohler, K., D. Louvard, and A. Zahraoui. 2004. Rab13 regulates PKA signaling during tight junction assembly. *J. Cell Biol.* 165:175–180.

Kuwabara, H., Y. Kokai, T. Kojima, R. Takakuwa, M. Mori, and N. Sawada. 2001. Occludin regulates actin cytoskeleton in endothelial cells. *Cell Struct. Funct.* 26:109–116.

Lapierre, L.A., P.L. Tuma, J. Navarre, J.R. Goldenring, and J.M. Anderson. 1999. VAP-33 localizes to both an intracellular vesicle population and with occludin at the tight junction. *J. Cell Sci.* 112:3723–3732.

Li, D., and R.J. Mrsny. 2000. Oncogenic Raf-1 disrupts epithelial tight junctions via downregulation of occludin. *J. Cell Biol.* 148:791–800.

Li, Y., A.S. Fanning, J.M. Anderson, and A. Lavie. 2005. Structure of the conserved cytoplasmic C-terminal domain of occludin: identification of the ZO-1 binding surface. *J. Mol. Biol.* 352:151–164.

Lynch, R.D., L.J. Tkachuk, X. Ji, C.A. Rabito, and E.E. Schneeberger. 1993. Depleting cell cholesterol alters calcium-induced assembly of tight junctions by monolayers of MDCK cells. *Eur. J. Cell Biol.* 60:21–30.

Martin-Padura, I., S. Lostaglio, M. Schneemann, L. Williams, M. Romano, P. Fruscella, C. Panzeri, A. Stoppacciaro, L. Ruco, A. Villa, et al. 1998.

Junctional adhesion molecule, a novel member of the immunoglobulin superfamily that distributes at intercellular junctions and modulates monocyte transmigration. *J. Cell Biol.* 142:117–127.

Mitic, L.L., and J.M. Anderson. 1998. Molecular architecture of tight junctions. *Annu. Rev. Physiol.* 60:121–142.

Ohnishi, H., T. Nakahara, K. Furuse, H. Sasaki, S. Tsukita, and M. Furuse. 2004. JACOP, a novel plaque protein localizing at the apical junctional complex with sequence similarity to cingulin. *J. Biol. Chem.* 279:46014–46022.

Patterson, G.H., and J. Lippincott-Schwartz. 2002. A photoactivatable GFP for selective photolabeling of proteins and cells. *Science.* 297:1873–1877.

Peng, B.H., J.C. Lee, and G.A. Campbell. 2003. In vitro protein complex formation with cytoskeleton-anchoring domain of occludin identified by limited proteolysis. *J. Biol. Chem.* 278:49644–49651.

Rajasekaran, A.K., M. Hojo, T. Huima, and E. Rodriguez-Boulan. 1996. Catenins and zonula occludens-1 form a complex during early stages in the assembly of tight junctions. *J. Cell Biol.* 132:451–463.

Saitou, M., M. Furuse, H. Sasaki, J.D. Schulzke, M. Fromm, H. Takano, T. Noda, and S. Tsukita. 2000. Complex phenotype of mice lacking occludin, a component of tight junction strands. *Mol. Biol. Cell.* 11:4131–4142.

Sakakibara, A., M. Furuse, M. Saitou, Y. Ando-Akatsuka, and S. Tsukita. 1997. Possible involvement of phosphorylation of occludin in tight junction formation. *J. Cell Biol.* 137:1393–1401.

Sasaki, H., C. Matsui, K. Furuse, Y. Mimori-Kiyosue, M. Furuse, and S. Tsukita. 2003. Dynamic behavior of paired claudin strands within apposing plasma membranes. *Proc. Natl. Acad. Sci. USA.* 100:3971–3976.

Schmidt, A., D.I. Utepbergenov, G. Krause, and I.E. Blasig. 2001. Use of surface plasmon resonance for real-time analysis of the interaction of ZO-1 and occludin. *Biochem. Biophys. Res. Commun.* 288:1194–1199.

Schulzke, J.D., A.H. Gitter, J. Mankertz, S. Spiegel, U. Seidler, S. Amasheh, M. Saitou, S. Tsukita, and M. Fromm. 2005. Epithelial transport and barrier function in occludin-deficient mice. *Biochim. Biophys. Acta.* 1669:34–42.

Schwarz, B.T., F. Wang, L. Shen, D.R. Clayburgh, L. Su, Y. Wang, Y.X. Fu, and J.R. Turner. 2007. LIGHT signals directly to intestinal epithelia to cause barrier dysfunction via cytoskeletal and endocytic mechanisms. *Gastroenterology.* 132:2383–2394.

Seth, A., P. Sheth, B.C. Elias, and R. Rao. 2007. Protein phosphatases 2A and 1 interact with occludin and negatively regulate the assembly of tight junctions in the CACO-2 cell monolayer. *J. Biol. Chem.* 282:11487–11498.

Shen, L., and J.R. Turner. 2005. Actin depolymerization disrupts tight junctions via caveolae-mediated endocytosis. *Mol. Biol. Cell.* 16:3919–3936.

Stevenson, B.R., J.D. Siliciano, M.S. Mooseker, and D.A. Goodenough. 1986. Identification of ZO-1: a high molecular weight polypeptide associated with the tight junction (Zonula Occludens) in a variety of epithelia. *J. Cell Biol.* 103:755–766.

Tang, V.W., and D.A. Goodenough. 2003. Paracellular ion channel at the tight junction. *Biophys. J.* 84:1660–1673.

Tomson, F.L., A. Koutsouris, V.K. Viswanathan, J.R. Turner, S.D. Savkovic, and G. Hecht. 2004. Differing roles of protein kinase C-zeta in disruption of tight junction barrier by enteropathogenic and enterohemorrhagic *Escherichia coli*. *Gastroenterology.* 127:859–869.

Tsukita, S., M. Furuse, and M. Itoh. 2001. Multifunctional strands in tight junctions. *Nat. Rev. Mol. Cell Biol.* 2:285–293.

Umeda, K., J. Ikenouchi, S. Katahira-Tayama, K. Furuse, H. Sasaki, M. Nakayama, T. Matsui, S. Tsukita, and M. Furuse. 2006. ZO-1 and ZO-2 independently determine where claudins are polymerized in tight-junction strand formation. *Cell.* 126:741–754.

Van Itallie, C.M., and J.M. Anderson. 1997. Occludin confers adhesiveness when expressed in fibroblasts. *J. Cell Sci.* 110:1113–1121.

Van Itallie, C.M., and J.M. Anderson. 2004. The molecular physiology of tight junction pores. *Physiology (Bethesda).* 19:331–338.

Wittchen, E.S., J. Haskins, and B.R. Stevenson. 1999. Protein interactions at the tight junction. Actin has multiple binding partners, and ZO-1 forms independent complexes with ZO-2 and ZO-3. *J. Biol. Chem.* 274:35179–35185.

Wong, V., and B.M. Gumbiner. 1997. A synthetic peptide corresponding to the extracellular domain of occludin perturbs the tight junction permeability barrier. *J. Cell Biol.* 136:399–409.

Yamada, S., S. Pokutta, F. Drees, W.I. Weis, and W.J. Nelson. 2005. Deconstructing the cadherin-catenin-actin complex. *Cell.* 123:889–901.

Ye, J., T. Tsukamoto, A. Sun, and S.K. Nigam. 1999. A role for intracellular calcium in tight junction reassembly after ATP depletion-repletion. *Am. J. Physiol.* 277:F524–F532.

Yguerabide, J., J.A. Schmidt, and E.E. Yguerabide. 1982. Lateral mobility in membranes as detected by fluorescence recovery after photobleaching. *Biophys. J.* 40:69–75.

Yu, A.S., K.M. McCarthy, S.A. Francis, J.M. McCormack, J. Lai, R.A. Rogers, R.D. Lynch, and E.E. Schneeberger. 2005. Knockdown of occludin expression leads to diverse phenotypic alterations in epithelial cells. *Am. J. Physiol. Cell Physiol.* 288:C1231–C1241.

Zahraoui, A., G. Joberty, M. Arpin, J.J. Fontaine, R. Hellio, A. Tavitian, and D. Louvard. 1994. A small rab GTPase is distributed in cytoplasmic vesicles in non polarized cells but colocalizes with the tight junction marker ZO-1 in polarized epithelial cells. *J. Cell Biol.* 124:101–115.